Effect of Sugar Palm-derived Cellulose Reinforcement on the Mechanical and Water Barrier Properties of Sugar Palm Starch Biocomposite Films

Muhammed Lamin Sanyang,[a] S. M. Sapuan,[a,b,c,*] Mohammad Jawaid,[c] Mohamad Ridzwan Ishak,[d] and Japar Sahari [e]

In this study, sugar palm-derived cellulose (SPC) composites were prepared and utilized as reinforcement material to improve the mechanical and water vapor barrier properties of sugar palm starch (SPS)-based films. Cellulose-reinforced SPS composite films (SPS-C) were prepared with different SPC loadings (1 to 10 wt.%) using a solution casting method. The mechanical properties of the composite films showed increased tensile strength and modulus, while the elongation at break decreased with SPC loading. Adding 1 wt. % SPC loading significantly improved the water vapor permeability (WVP) of the composite film by 63.53% compared with the neat SPS film. This was ascribed to the high compatibility between the SPC and SPS matrices, which was supported by the field emission scanning electron microscopy (FESEM) and Fourier transform infrared spectroscopy (FTIR) results.

Contact information: a: Green Engineering, Institute of Advanced Technology, Universiti Putra Malaysia, 43400 UPM Serdang, Selangor, Malaysia; b: Department of Mechanical and Manufacturing Engineering, Universiti Putra Malaysia, 43400 UPM Serdang, Selangor, Malaysia; c: Laboratory of Biocomposite Technology, Institute of Tropical Forestry and Forest Products, Universiti Putra Malaysia, 43400 UPM Serdang, Selangor, Malaysia; d: Department of Aerospace Engineering, Universiti Putra Malaysia, 43400 UPM Serdang, Selangor, Malaysia; e: Faculty of Science and Natural Resources, Universiti Malaysia Sabah, Jalan UMS, 88400 Kota Kinabalu, Sabah, Malaysia; *Corresponding author: sapuan@upm.edu.my

INTRODUCTION

The growing environmental devastation ascribed to the disposal of packaging plastic waste has led to an urgent need to develop environmentally friendly packaging materials to rescue our ecosystem (Kaushik *et al.* 2010). In an effort to resolve the ongoing environmental crisis caused by non-biodegradable plastics, natural biopolymers have been investigated as potential alternatives to conventional plastics. Starch is one of the most widely available biopolymers for packaging applications. In addition to its wide availability, it is affordable, renewable, and biodegradable. Therefore, starch has attracted a great deal of attention as a promising green material as well as a potential alternative to non-biodegradable plastics (Savadekar and Mhaske 2012).

However, starch-based films for packaging have been reported to have poor mechanical strength and a low water barrier resistance (Teixeira *et al.* 2009; Bilbao-Sainz *et al.* 2011; Teac *et al.* 2013). Such drawbacks strongly limit their wide application, especially for food packaging purposes. Many studies have been undertaken by material scientists to improve the mechanical properties and enhance the water sensitivity of starch-based materials without compromising their biodegradability (Sanchez-Garcia *et al.* 2008;

bioresources.com

Müller *et al.* 2009; Dias *et al.* 2011). The addition of natural cellulose fibers during the preparation of starch composite films is an effective strategy for improving the functional properties of packaging films, as documented by various researchers (Teixeira *et al.* 2009; Teac *et al.* 2013; Slavutsky and Bertuzzi 2014). Thus, green micro/nanocomposite films are envisaged as next-generation packaging materials.

Cellulose is a bio-based material abundantly found in natural plants. The cellulose commonly derived from cellulosic fibers is generated by plants through photosynthesis, using water and carbon dioxide in the presence of energy from sunlight (Ng *et al.* 2015). Cellulose is known to be the backbone material of the long fibrous cells embedded in hemicelluloses and lignin. The removal of hemicelluloses and lignin using different chemical treatment techniques was shown to give rise to a new, eco-friendly fiber material: cellulose microfibers. They are readily available, inexpensive, renewable, and lightweight (Kaushik *et al.* 2010). Cellulose fibers utilized as reinforcement have been shown to enhance the performance of starch composite films by providing high thermal stability and good mechanical properties such as high tensile strength and high Young's modulus (Kaushik *et al.* 2010; Savadekar and Mhaske 2012). Furthermore, the addition of cellulose fibers has been reported to decrease the water vapor permeability of starch-based films (Müller *et al.* 2009; Dias *et al.* 2011), thus increasing their suitability for food packaging applications.

Numerous types of cellulosic reinforcements have been investigated and tested in biopolymers. Interestingly, it was found that the compatibility between the starch matrix and cellulose fibers is high, which is significant for obtaining enhanced mechanical and water sensitivity (Kaushik *et al.* 2010). Based on previous studies (Ishak *et al.* 2013), sugar palm is considered to be a good source of cellulose fiber because of its high cellulose content.

Sugar palm is a multipurpose tree mostly grown in tropical countries. It serves as a potential source of natural fiber and starch for developing green composite materials. Several studies by the authors (Sanyang *et al.* 2015a,b, 2016) have reported on the physical, mechanical, thermal, and water barrier properties of plasticized sugar palm starch films for food packaging applications. The results obtained from these previous studies suggest upgrading the mechanical and water vapor barrier properties of sugar palm starch films to further enhance their performance.

To the best of our knowledge, no study on sugar palm-derived cellulose has been found in the literature. Hence, the aim of the current study was to extract cellulose from sugar palm fibers and incorporate the sugar palm-derived cellulose into sugar palm starch as reinforcement material to improve the mechanical and water vapor barrier properties of sugar palm-based films.

EXPERIMENTAL

Materials

Sugar palm starch and fibers were extracted from sugar palm trees at Jempol, Negeri Sembilan (Malaysia). Reagent-grade acetic acid (CH_3COOH), sodium hydroxide (NaOH), and technical-grade sodium chlorite ($NaClO_2$) of 80% purity were purchased from LGC Scientific Sdn Bhd (Selangor, Malaysia). Reagent-grade glycerol and sorbitol plasticizers were also obtained from the same supplier.

Sugar Palm Fiber Extraction and Preparation

Figure 1 shows the extraction and preparation process of the sugar palm fibers (SPF) used in this work. SPF were extracted from different parts of the sugar palm tree (sugar palm frond, bunch, ijuk, and trunk). The SPF is readily wrapped around the trunk of the tree from top to bottom. A slashing knife was utilized to manually remove SPF from the tree, and the harvested SPF required no secondary processing such as mechanical retting. In order to obtain uniform SPF size (2 mm), a Fritsch pulverisette mill was used for grinding and screening the SPF to the desired size.

Fig. 1. Extraction and preparation of SPF

Cellulose Extraction

In accordance with Tawakkal *et al.* (2012) and Tee *et al.* (2013), cellulose fibers were extracted from sugar palm fibers (SPF) using two main processes: delignification and mercerization. The initial process was performed in accordance with ASTM D1104-56 (1978) to prepare holocellulose through a chlorination or bleaching process, primarily designed for the removal of lignin from the SPF. In this step, 20 g of SPF was rinsed with tap water to remove dust and foreign particles. The clean SPF was soaked in a 1000-mL beaker containing 650 mL of hot distilled water, which was subsequently transferred to a water bath, and the temperature was set at 70 °C. Thereafter, 4 mL of acetic acid and 8 g of sodium chlorite were added to the beaker every hour for 5 h, consecutively. The changing color of the SPF from light brown to white indicated the level of delignification. The obtained celluloses are referred to as holocellulose and were filtered, washed, and rinsed with distilled water.

The holocellulose was further treated to produce alpha-cellulose according to ASTM D1103-60 (1977). The holocellulose was soaked in 500 mL of 5% w/v NaOH solution for 2 h at 23 ± 2 °C. The alpha-cellulose produced was filtered and immersed in 500 mL of distilled water containing approximately 7 mL of acetic acid to neutralize the cellulose. The mixture was stirred for approximately 30 s before it was allowed to settle for 5 min. Therefore, the cellulose was rinsed with water until the cellulose residue was free from acid, as indicated by a pH meter. Lastly, the cellulose denoted as SPC in the current study was dried in an oven at 103 °C overnight.

Preparation of Composite Films

The composite films were developed using a solution casting technique. An aqueous suspension of SPC was prepared by mixing known concentrations of SPC (1 to 10 wt. % on a starch basis) with distilled water. The starch-film-forming solution was prepared by adding 10 g of SPS to 125 mL of distilled water. Cellulose fibers were added

to the SPS film-forming mixture and stirred at 1000 rpm for 20 min in a disperser. Thereafter, 30% of combined glycerol and sorbitol (1:1 combination of glycerol and sorbitol ratio) as a single plasticizer was added to the mixture under constant stirring (100 rpm) while the mixture was heated at 95 °C for 15 min. The film-forming suspension was left to cool before 35 g of the suspension was poured into each petri dish (13-cm diameter). The dishes containing the film-forming solution were placed in an oven at 40 °C for 24 h. SPS films prepared without SPC served as the control (denoted as SPS   films). Composite films with 1, 3, 5, and 10 wt.% SPC were designated as SPS-C1, SPS-C3, SPS-C5, and SPS-C10, respectively.

FESEM

The morphology of raw sugar palm fiber and sugar palm-derived cellulose was investigated using a field emission scanning electron microscope (JEOL JSM-7600F, Japan) at an acceleration voltage of 5 kV. The film samples were mounted on aluminum stubs with double-sided adhesive tape. Thereafter, the samples were coated with gold to avoid charging using an argon plasma metallizer (sputter coater PELCO 91000). Digital image analysis (Image J) was utilized to examine the diameter of both samples.

FTIR

Infrared spectra of the film samples were analyzed using Fourier transform infrared spectroscopy in attenuated total reflectance mode (FTIR-ATR). First, a film sample was mounted on a sample holder in contact with ZnSe crystal and then placed on an attenuated total reflectance accessory. FTIR spectra were collected by recording 42 scans with a resolution of 4 cm^{-1} in a 4000 to 400 cm^{-1} wave range. The ZnSe crystal, which possesses a high reflectivity index, was thoroughly cleaned after each measurement.

Tensile Properties

An Instron 3365 universal testing machine (High Wycombe, England) with a loading cell of 30 kg was used to determine the tensile properties of film samples. The film samples were tested, as suggested by Sanyang *et al.* (2015b), and the tensile strength and elongation at break were determined according to the standard method ASTM D882 (2002). The films were cut into strips with dimensions of 10 mm $\times$ 70 mm. The strips were clamped between two tensile grips and the initial gauge length was set at 30 mm. The films were pulled using a crosshead speed of 2 mm/min. During the stretching, the values of force (N) and deformation (mm) were recorded. Measurements were taken from 10 different specimens. The mechanical properties were calculated as the average value of the obtained results. It is worth mentioning that the effects of rheological parameters on the mechanical properties were not considered in the current study.

Water Vapor Permeability (WVP)

Prior to the WVP test, the film samples were conditioned in a desiccator with a relative humidity of 50% at 25 °C. The WVP test was conducted according to ASTM E96 (1995), with slight modifications according to Sanyang *et al.* (2015b). Circular film samples were placed over and sealed on the mouth of the test cup which has 30 mm diameter. The test cups were prefilled with 20 g of silica gel, leaving about 3 mm vacuum to the top. Thereafter, the test cups were weighed before keeping in a relative humidity chamber (25 °C, relative humidity 75%). Weight gain values of the cups were measured

periodically until the equilibrium state was reached. Weight increments of the test cups were recorded, and WVP was calculated as follows,

$$WVP = \frac{(m \times d)}{(A \times t \times P)} \tag{1}$$

where m (g) is the weight increment of the test cup, d (mm) is the film thickness, A (m^2) is the area of film exposed, t (s) is the duration of permeation, and P (Pa) is the water vapor partial pressure across the films. The results are expressed in g mm s^{-1} m^{-2} Pa^{-1}. This experiment was replicated thrice.

Statistical Analysis

Statistical analyses of the obtained experimental results were performed by analysis of variance (ANOVA) using Minitab 16 software (Minitab Pty Ltd., Sydney, Australia). Mean comparisons were conducted using Tukey's test at a 0.05 level of significance ($p \leq 0.05$).

RESULTS AND DISCUSSION

Morphology of SPC

FESEM micrographs of sugar palm fiber (SPF) and sugar palm-derived cellulose (SPC) (Fig. 2) revealed their homogeneity and micrometric dimensions. The average diameters of SPF and SPC were approximately 43.71 ± 9 μm and 10.24 ± 3 μm, respectively. This clearly indicates that the diameter of SPC was almost four times smaller than that of SPF. The obtained diameter for SPC is in agreement with the average diameter of kenaf-derived cellulose (13 μm) reported by Tawakkal *et al.* (2012). Elsewhere, Sonia *et al.* (2013) reported 10.04 μm to be the average diameter of cellulose microfibers. In a separate investigation, Tee *et al.* (2013) also reported that the diameter of kenaf-derived cellulose (17.38 μm) was four times smaller than that of the natural kenaf fiber (61.77 μm). The drastic reduction in the diameter of SPC can be attributed to the removal of hemicellulose and lignin through the delignification and mercerization of raw SPF.

It can be seen that the surface topography of the rod-like SPFs is rough, with pore-like spots that appear in almost regular intervals. Similar spots were reported by Ticoalu *et al.* (2012) with respect to the surface of sugar palm fibers and coir. According to their report, these visible spots on the surface of the fibers are known as tyloses, which cover the pits on the cell walls. Nevertheless, after removing the hemicellulose and lignin of SPF, the derived SPC had a relatively smooth surface, with parallel lines running along the length of the cellulose. Thus, the topography of SPC can be described as a groovy surface. Similar reports have been documented regarding the surface appearance of many natural fiber-derived celluloses (Sgriccia *et al.* 2008; Tawakkal *et al.* 2012; Tee *et al.* 2013).
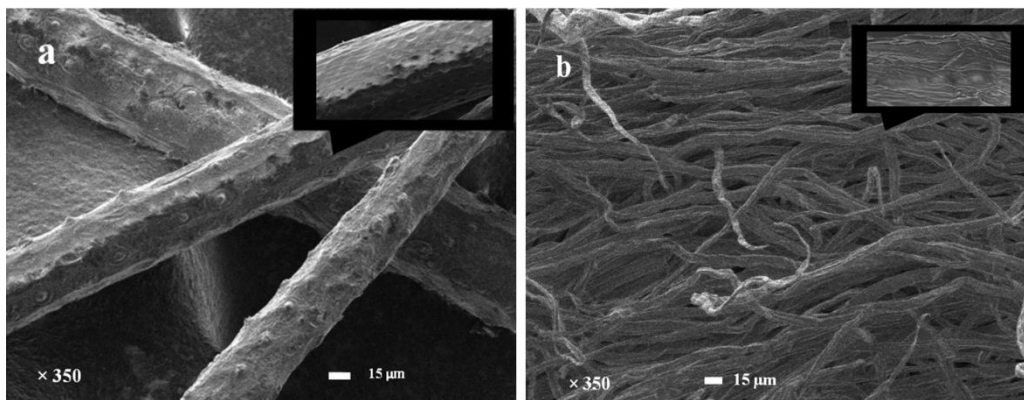
Fig. 2. FESEM micrographs of (a) raw sugar palm fiber and (b) sugar palm-derived cellulose
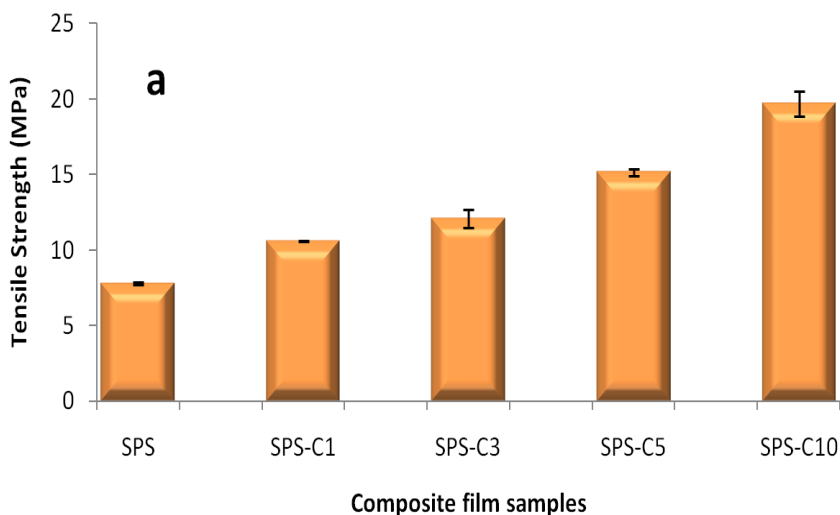
FTIR of Composite Films

Figure 3 shows the infrared (IR) spectra of neat SPS and SPS-C composite films with different SPC concentrations. The broad peak of the SPS film observed at 3600 to 3020 cm^{-1} corresponded to the O–H group, whereas the peak at 2950 cm^{-1} was assigned to C–H stretching. The small peak displayed at 1680 cm^{-1} was attributed to C=O stretching. The band at 1305 cm^{-1} was related to the O–H of water. A similar peak was reported by Bourtoom and Chinnan (2008) with rice starch film. The sharp peak at 1004 cm^{-1} was associated with the C–O bond of C–O–C groups. The neat SPS film demonstrated a similar IR spectrum compared with the SPS-C composite films, irrespective of SPC concentration. The addition of SPC shows an insignificant effect on the IR spectrum of SPS films because of the lack of new peaks. This phenomenon manifested in the SPC and SPS matrices, which have similar chemical groups and thus indicates a potential compatibility between the two components. Alternatively, the similarity between the IR spectra of SPS-based films before and after SPC reinforcement could exist because both SPS and SPC originated from a single source (sugar palm tree).
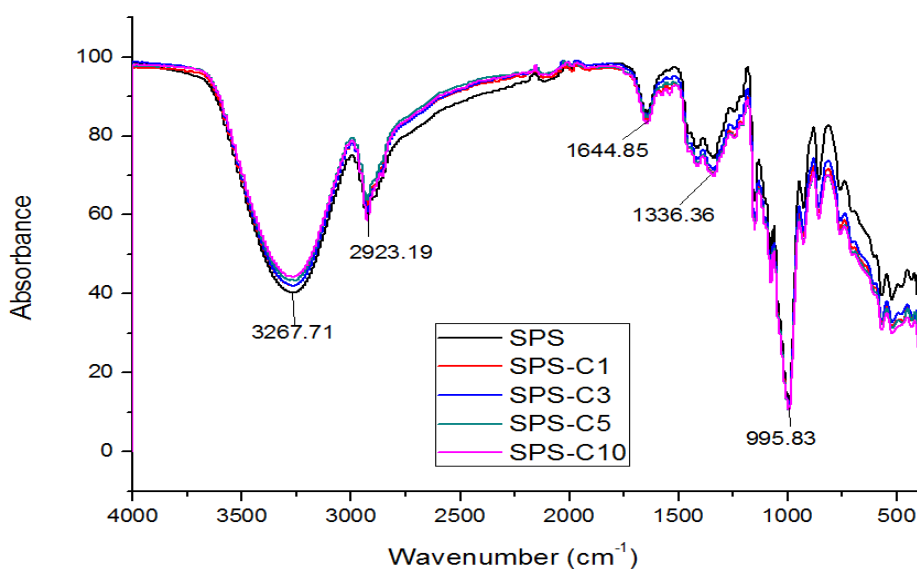

Fig. 3. IR spectra of neat SPS and SPS-C composite films

bioresources.com

Tensile Properties

The effect of SPC loading on the tensile strength, tensile modulus, and elongation at break of SPS-based composite films were determined and the results are presented in Fig. 4. As expected, it is apparent that the tensile strength, and tensile modulus of SPS-C composite films increased as the SPC concentration increased from 1 to 10 wt.%. The tensile strength and tensile modulus of the neat SPS films were 7.79 and 20.11 MPa, respectively. Adding 1 to 10 wt.% SPC reinforcement significantly increased the tensile strength and tensile modulus values of the composite films (from 10.5 to 19.68 MPa and from 31.38 to 92.33 MPa, respectively). Hence, at the maximum SPC loading (10 wt.%), the tensile strength of SPS-C10 improved by 60.42%, while the tensile modulus was 78.22% higher than that of the neat SPS film. This observed tensile behavior can be attributed to the favorable interaction between the SPC and SPS matrices, which facilitated adequate interfacial adhesion because of their chemical similarities. Similar results were reported by other authors (Dias _et al._ 2011; Pereda _et al._ 2011). In addition, contrary to the increase in tensile strength and tensile modulus, the elongation at break for the composite films decreased from 40.99 to 32.8% as the SPC concentration increased from 1 to 10 wt.% in the neat SPS films. This marks a reduction in elongation at break of approximately 30% for SPS-C10 composite films compared with neat SPS films. The introduction and increase of SPC decreased the molecular mobility of the SPS matrix, making the composite materials stiffer. Therefore, SPS-C composite films became more resistant to break, stiffer, and less stretchable than the virgin SPS films.
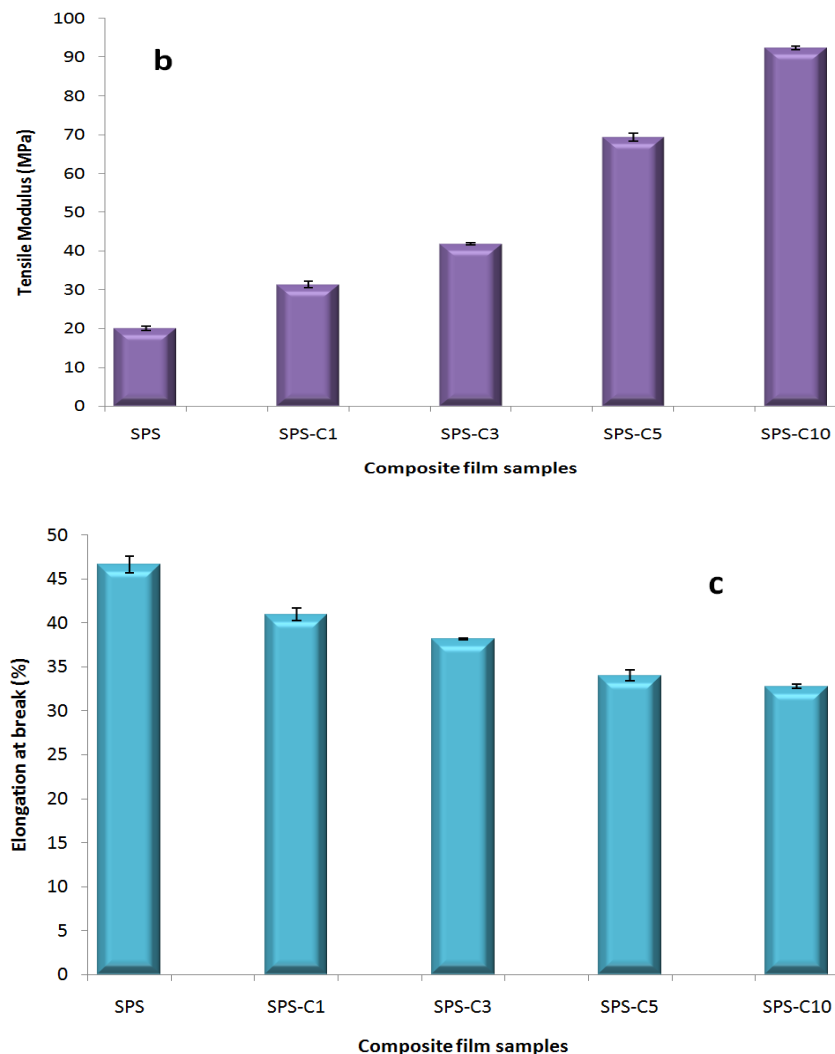
Fig. 4. Effect of SPC loading on the (a) tensile strength, (b) tensile modulus, and (c) elongation at break of SPS-C composite films compared with neat SPS films

Water Vapor Permeability

Films with low WVP are suitable for food packaging applications, including the prevention or minimization of moisture transfer between food and the surrounding environment. Therefore, reducing the WVP of SPS films is crucial for their wide application. The WVP of neat SPS and SPS-C composite films are presented in Fig. 5. It can be seen that the SPS films had the highest WVP ($6.373 \times 10^{-10} \times$ g·s^{-1}·m^{-1}·Pa^{-1}) because of its highly hydrophilic nature. The presence of SPC drastically improved the WVP of the neat SPS films. The addition of 1% SPC into SPS films decreased their WVP value by 63.53%. This reduction can be attributed to the tortuous path caused by the dispersed SPC in the starch matrix, which hinders or prolongs the path through which the water molecules pass. Increasing the SPC concentration from 1 to 10 wt.% caused a slight decrease in the WVP of composite films from $2.324 \times 10^{-10} \times$ g·s^{-1}·m^{-1}·Pa^{-1} to $1.854 \times 10^{-10} \times$ g·s^{-1}·m^{-1}·Pa^{-1}. Thus, SPS-C10 films displayed a 70.91% improvement in WVP compared with neat SPS films.
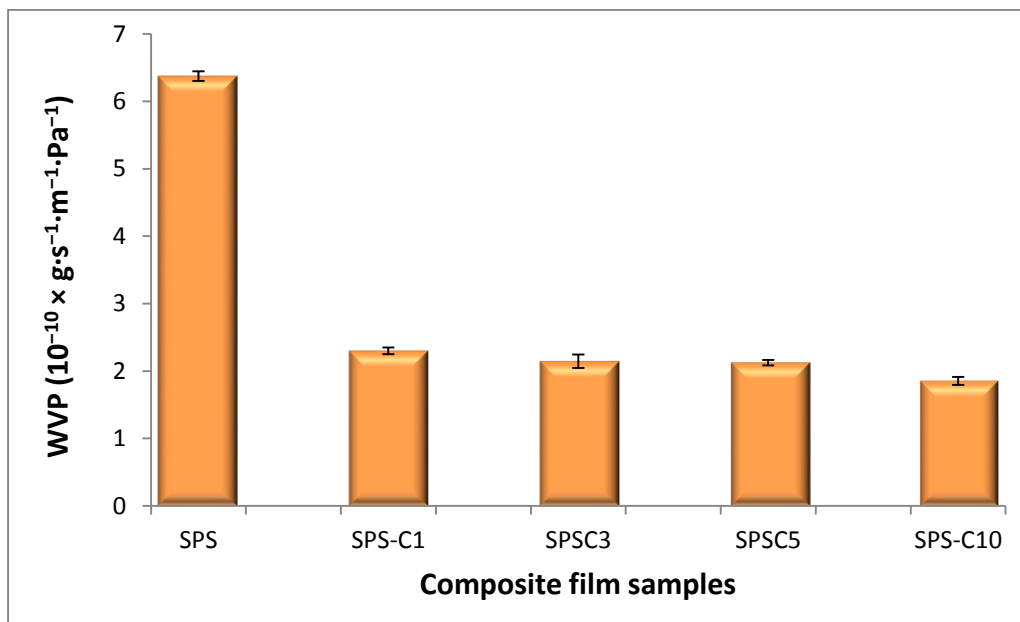
Fig. 5. Effect of SPC loading on the WVP of SPS-C composite films compared with neat SPS films

Surface Morphology of Composite Films

Figure 6 shows the FESEM images of the surface morphology of SPS-based films with and without the addition of SPC. The micrograph of the virgin SPS films showed a smooth and continuous surface with no trace of starch granular or cracks. Similar observations were reported by Sanyang *et al.* (2016) and Dias *et al.* (2011) for neat sugar palm starch and rice flour films, respectively. On the other hand, the addition of 10 wt.% SPC to a virgin SPS film (SPS-C10) displayed an even, random distribution of SPC within the SPS matrix, without pores or cracks. However, the SPS-C10 composite film surface became rougher, with some of the SPC fibers overlapping, but with no noticeable clusters or agglomerations of SPC. Therefore, the high dispersion of SPC (Fig. 6(b)) is a good indication of strong interfacial adhesion between the two components of the SPS-C10 film. This strong interfacial adhesion translates into high tensile strength. These findings concur with those reported by Bilbao-Sainz *et al.* (2011) and Savadekar and Mhaske (2012). In fact, Bilbao-Sainz *et al.* (2011) reported that cellulose fibers must be well-dispersed into the polymeric matrix to enhance the functional properties of the composite.
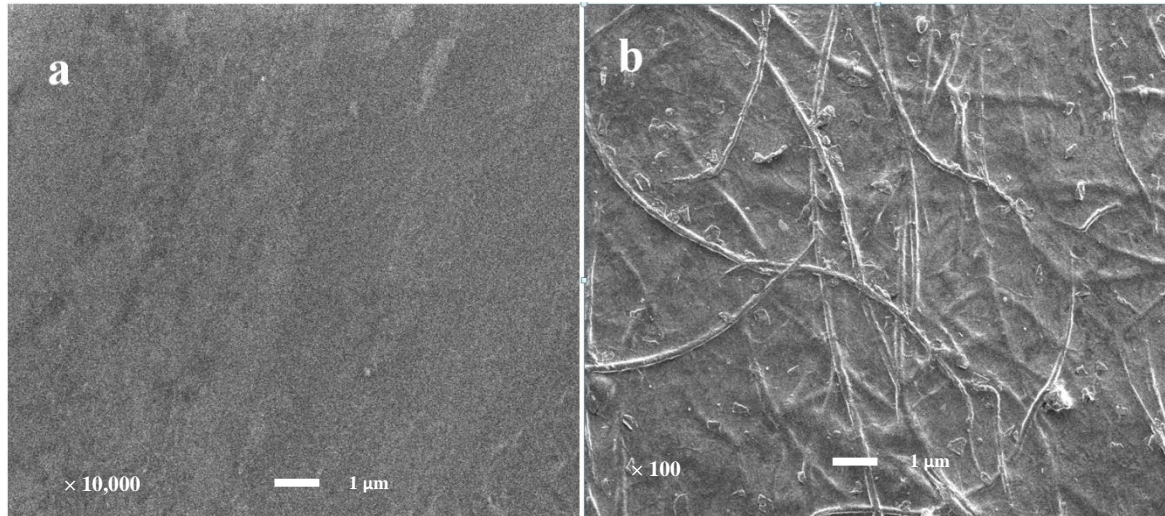
Fig. 6. FESEM micrographs of (a) neat SPS film and (b) SPS-C10 film

CONCLUSIONS

1. SPC was extracted from sugar palm fibers using the methods of delignification and mercerization. The effects of SPC loading on the mechanical and water vapor barrier properties of SPS-based films were successfully evaluated.

2. The mechanical properties, including tensile strength, tensile modulus, and elongation at break, as well as the water vapor permeability (WVP) of the SPS-C composite films were analyzed. The addition of SPC considerably improved the overall mechanical properties and water vapor barrier of the composite films.

3. FESEM micrographs showed an adequate, random dispersion of SPC into the SPS matrix. This was attributed to the high compatibility between the two components as a result of their chemical similarities. Hence, this study illuminated the great potential of SPS-C composite films for packaging applications.

ACKNOWLEDGMENTS

REFERENCES CITED

ASTM D1104-56 (1978). "Method of test for holocellulose in wood," American Society for Testing and Materials, USA.

ASTM D1103-60 (1977). "Method of test for alpha-cellulose in wood," American Society for Testing and Materials, USA.

bioresources.com

ASTM D882 (2002). "Standard test method for tensile properties of thin plastic sheeting," American Society for Testing and Materials, USA.

ASTM E96 (1995). "Standard Test method for water vapor transmission of materials," American Society for Testing and Materials, USA.

Bilbao-Sainz, C., Bras, J., Williams, T., Sénechal, T., and Orts, W. (2011). "HPMC reinforced with different cellulose nano-particles," _Carbohydrate Polymers_ 86(4), 1549-1557. DOI: 10.1016/j.carbpol.2011.06.060

Bourtoom, T., and Chinnan, M. S. (2008). "Preparation and properties of rice starch–chitosan blend biodegradable film," _LWT-Food Science and Technology_ 41(9), 1633-1641. DOI: 10.1016/j.lwt.2007.10.014

Dias, A. B., Müller, C. M. O., Larotonda, F. D. S., and Laurindo, J. B. (2011). "Mechanical and barrier properties of composite films based on rice flour and cellulose fibers," _LWT-Food Science and Technology_ 44(2), 535-542. DOI: 10.1016/j.lwt.2010.07.006

Ishak, M. R., Sapuan, S. M., Leman, Z., Rahman, M. Z. A., Anwar, U. M. K., and Siregar, J. P. (2013). "Sugar palm (_Arenga pinnata_): Its fibres, polymers and composites," _Carbohydrate Polymers_ 91(2), 699-710. DOI: 10.1016/j.carbpol.2012.07.073

Kaushik, A., Singh, M., and Verma, G. (2010). "Green nanocomposites based on thermoplastic starch and steam exploded cellulose nanofibrils from wheat straw," _Carbohydrate Polymers_ 82(2), 337-345. DOI: 10.1016/j.carbpol.2010.04.063

Müller, C. M. O., Laurindo, J. B., and Yamashita, F. (2009). "Effect of cellulose fibers addition on the mechanical properties and water vapor barrier of starch-based films," _Food Hydrocolloids_ 23(5), 1328-1333. DOI: 10.1016/j.foodhyd.2008.09.002

Ng, H.-M., Sin, L. T., Tee, T.-T., Bee, S.-T., Hui, D., Low, C.-Y., and Rahmat, A. R. (2015). "Extraction of cellulose nanocrystals from plant sources for application as reinforcing agent in polymers," _Composites Part B: Engineering_ 75, 176-200. DOI: 10.1016/j.compositesb.2015.01.008

Pereda, M., Amica, G., Rácz, I., and Marcovich, N. E. (2011). "Preparation and characterization of sodium caseinate films reinforced with cellulose derivatives," _Carbohydrate Polymers_ 86(2), 1014-1021. DOI: 10.1016/j.carbpol.2011.05.063

Sanchez-Garcia, M. D., Gimenez, E., and Lagaron, J. M. (2008). "Morphology and barrier properties of solvent cast composites of thermoplastic biopolymers and purified cellulose fibers," _Carbohydrate Polymers_ 71(2), 235-244. DOI: 10.1016/j.carbpol.2007.05.041

Sanyang, M. L., Sapuan, S. M., Jawaid, M., Ishak, M. R., and Sahari, J. (2016). "Effect of plasticizer type and concentration on physical properties of biodegradable films based on sugar palm (_Arenga pinnata_) starch for food packaging," _Journal of Food Science and Technology_ 53(1), 326-336.

Sanyang, M. L., Sapuan, S. M., Jawaid, M., Ishak, M. R., and Sahari, J. (2015a). "Effect of plasticizer type and concentration on dynamic mechanical properties of sugar palm starch based films," _International Journal of Polymer Analysis and Characterization_ 20(7), 627-636. DOI: 10.080/1023666X.2015.1054107

Sanyang, M. L., Sapuan, S., Jawaid, M., Ishak, M., and Sahari, J. (2015b). "Effect of plasticizer type and concentration on tensile, thermal and barrier properties of biodegradable films based on sugar palm (_Arenga pinnata_) starch," _Polymers_ 7(6), 1106-1124. DOI: 10.3390/polym7061106

bioresources.com

Savadekar, N. R., and Mhaske, S. T. (2012). "Synthesis of nano cellulose fibers and effect on thermoplastics starch based films," *Carbohydrate Polymers* 89(1), 146-151. DOI: 10.1016/j.carbpol.2012.02.063

Sgriccia, N., Hawley, M. C., and Misra, M. (2008). "Characterization of natural fiber surfaces and natural fiber composites," *Composites Part A: Applied Science and Manufacturing* 39(10), 1632-1637. DOI: 10.1016/j.compositesa.2008.07.007

Slavutsky, A. M., and Bertuzzi, M. A. (2014). "Water barrier properties of starch films reinforced with cellulose nanocrystals obtained from sugarcane bagasse," *Carbohydrate Polymers* 110, 53-61. DOI: 10.1016/j.carbpol.2014.03.049

Sonia, A., Priya Dasan, K., and Alex, R. (2013). "Celluloses microfibres (CMF) reinforced poly (ethylene-co-vinyl acetate) (EVA) composites: Dynamic mechanical, gamma and thermal ageing studies," *Chemical Engineering Journal* 228, 1214-1222. DOI: 10.1016/j.cej.2013.04.091

Tawakkal, I. S. M. A., Talib, R. A., Abdan, K., and Ling, C. N. (2012). "Mechanical and physical properties of kenaf-derived cellulose (KDC)-filled polylactic acid (PLA) composites," *BioResources* 7(2), 1643-1655. DOI: 10.15376/biores.7.2.1643-1655

Teac, C., Bodîrl, R., and Spiridon, I. (2013). "Effect of cellulose reinforcement on the properties of organic acid modified starch microparticles/plasticized starch bio-composite films," *Carbohydrate Polymers* 93, 307-315. DOI: 10.1016/j.carbpol.2012.10.020

Tee, Y. B., Talib, R. A., Abdan, K., Chin, N. L., Basha, R. K., and Md Yunos, K. F. (2013). "Thermally grafting aminosilane onto kenaf-derived cellulose and its influence on the thermal properties of poly(lactic acid) composites," *BioResources* 8(3), 4468-4483. DOI: 10.15376/biores.8.3.4468-4483

Teixeira, E. D. M., Pasquini, D., Curvelo, A. A. S., Corradini, E., Belgacem, M. N., and Dufresne, A. (2009). "Cassava bagasse cellulose nanofibrils reinforced thermoplastic cassava starch," *Carbohydrate Polymers* 78(3), 422-431. DOI: 10.1016/j.carbpol.2009.04.034

Ticoalu, A., Aravinthan, T., and Cardona, F. (2012). "A review on the characteristics of gomuti fibre and its composites with thermoset resins," *Journal of Reinforced Plastics and Composites* 32(2), 124-136. DOI: 10.1177/0731684412463109